AD-A121 640 A STUDY OF SECULAR AND TIDAL TILT IN WYOMING AND UTAH 1/1
(U) COLORADOUUNIV AT BOULDER J LEVINE ET AL. 15 SEP 82
AFGL-TR-82-0303 F19628-81-K-0040

UNCLASSIFIED F/G 8/7 NL

END
FILMED
DTIC

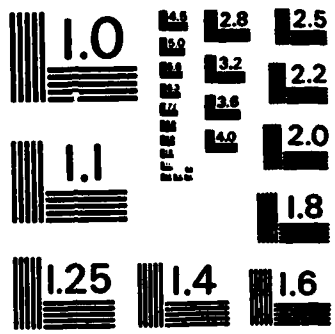
1.0
1.1
1.25
1.4
1.6
1.8
2.0
2.2
2.5
2.8
3.2
3.6
4.0

AD A121640

AFGL-TR-82-0303

A STUDY OF SECULAR AND TIDAL TILT IN WYOMING AND UTAH

Judah Levine
J.C. Harrison

The University of Colorado
Campus Box 440
Boulder, Colorado 80309

Scientific Report No. 1

15 September 1982

Approved for public release; distribution unlimited

AIR FORCE GEOPHYSICS LABORATORY
AIR FORCE SYSTEMS COMMAND
UNITED STATES AIR FORCE
HANSCOM AFB, MASSACHUSETTS 01731

82 11 22 176

Unclassified

SECURITY CLASSIFICATION OF THIS PAGE (When Data Entered)

REPORT DOCUMENTATION PAGE

READ INSTRUCTIONS BEFORE COMPLETING FORM

1. REPORT NUMBER AFGL-TR-82-0303	2. GOVT ACCESSION NO. AD-A121640	3. RECIPIENT'S CATALOG NUMBER
4. TITLE (and Subtitle) A STUDY OF SECULAR AND TIDAL TILT IN WYOMING AND UTAH		5. TYPE OF REPORT & PERIOD COVERED Scientific Report No. 1
		6. PERFORMING ORG. REPORT NUMBER
7. AUTHOR(s) Judah Levine J.C. Harrison		8. CONTRACT OR GRANT NUMBER(s) F19628-81-K-0040
9. PERFORMING ORGANIZATION NAME AND ADDRESS The University of Colorado Campus Box 440 Boulder, Colorado 80399		10. PROGRAM ELEMENT, PROJECT, TASK AREA & WORK UNIT NUMBERS 61102F 2309G2AJ
11. CONTROLLING OFFICE NAME AND ADDRESS Air Force Geophysics Laboratory Hanscom AFB, Massachusetts 01731 Monitor/Gerry Cabaniss/LWH		12. REPORT DATE 15 September 1982
		13. NUMBER OF PAGES 19
14. MONITORING AGENCY NAME & ADDRESS(if different from Controlling Office)		15. SECURITY CLASS. (of this report) Unclassified
		15a. DECLASSIFICATION/DOWNGRADING SCHEDULE

16. DISTRIBUTION STATEMENT (of this Report)

Approved for public release; distribution unlimited

17. DISTRIBUTION STATEMENT (of the abstract entered in Block 20, if different from Report)

18. SUPPLEMENTARY NOTES

19. KEY WORDS (Continue on reverse side if necessary and identify by block number)

Earth tides
Tiltmeter
Hydrofracture
Tidal admittance

were used

20. ABSTRACT (Continue on reverse side if necessary and identify by block number)

During the period covered by this report, we have used our borehole tiltmeter arrays to measure the tidal admittance at our two sites and to study the long-term performance of our instruments. These studies have resulted in several improvements to our original design. We were also fortunate in being able to monitor the surface tilting resulting from a nearby hydro-fracture experiment near our Erie site. The parameters of the hydro-fracture experiment as deduced from the tilt record are in reasonable

DD FORM 1 JAN 73 1473 EDITION OF 1 NOV 65 IS OBSOLETE

Unclassified

SECURITY CLASSIFICATION OF THIS PAGE (When Data Entered) agreement with simple models of the region. (The hydro-fracture experiment was not planned. We undertook it only when we discovered the pumping crew in the field South of our Erie array.) During the period covered by this report, we also completed the design of the Yellowstone array and began its construction. We have presented details of our design in our quarterly progress reports, and we shall only discuss it briefly here.

SUMMARY OF OBJECTIVES

1. To conduct field and laboratory measurements of long term crustal tilt at periods longer than four minutes.

2. To deploy an array of instruments in Yellowstone National Park to study the effect of the thermal anomaly on the tidal admittance.

3. To deploy an array of instruments near Ogden, Utah to study the secular tilt along the Wasatch fault zone. This is a seismically active region with a possible seismic gap near Ogden.

INTRODUCTION

During the first grant period, we designed several different types of tiltmeters. All of the instruments were built using various types of sensors purchased from INSTECH. We also drilled two sets of boreholes -- four holes of varying depth in Boulder, Colorado on the Department of Commerce site and five holes near Erie, Colorado on a section owned by the Government.

At the start of the current grant period, both arrays were operating continuously, although the number of active instruments at each site fluctuated from time to time. The data were sent via telephone lines and radio links to our laboratory on the campus of the University where we performed our analyses.

During the past year, we have evaluated our system by making detailed measurements of the tidal admittance at the various sites. We have also looked at the sensitivity of the instruments to various spurious effects such as rainfall and barometric pressure.

The results of these investigations have been quite encouraging: we find good agreement between theory and experiment. The details of our experiments are presented below.

EARTH TIDE RESULTS

Throughout the course of our work, we have always chosen to use the stability of the earth-tide admittance as a measure of the performance of our instruments.

The tidal admittance is calculated in several steps:

1. The data recorded by the various instruments are first broken into nominal 1-month segments. This length is chosen to achieve a reasonable separation among the tidal components. Although we have used shorter lengths of record, the results of these analyses of shorter records are often quite misleading when Fourier spectra are examined since tidal effects and thermal effects are not well resolved.

2. Each data set is then patched to yield a continuous time series at the original sampling interval (10 samples/hour). Short gaps in the data (up to a few hours long) are patched by simple linear interpolation. There are usually several of these per month. They are usually caused either by power failures at the tiltmeter or by a failure of the central computer. Longer gaps require a more detailed patching procedure. The amplitudes of the largest tidal constituents are estimated immediately before and after the gap; the resultant amplitudes and phases are used to construct a patched time series. The mean value of the patched series is adjusted to match the average of the values at the end points. If the values at the end points are significantly different (i.e., if the difference is greater than 1% of the tidal amplitude), the offset is removed by adding a sloping baseline to the patched series. If the gap is shorter than a few

days, this procedure works very well. The secular tilt rate is quite small and it is usually very close to a linear function of time. (We have never seen a tilt "episode" on any tiltmeter unless it was broken). Although this process is tedious, it is not necessary very often. There are usually only one or two such gaps per month.

3. The data are then lowpass-filtered using a symmetric lead-lag filter with a corner frequency near 1 cycle/hour; the filtered time series is decimated to one or two samples per hour for further analysis. The filter not only reduces the size of the data set thereby easing the subsequent analysis, but also removes the small residual "rough-edges" that are often present at the patch points (no patching process can ever be perfect since the addititve noise present in the data is not present in the patch).

4. The admittance is then estimated by fitting the tidal time series with an expansion of the tidal potential in spherical harmonics. This is a linear least-squares procedure. We usually allow the tidal admittance to have 4 degrees of freedom: an amplitude and phase in the diurnal band and an amplitude and phase in the semidiurnal band. In addition, we usually fit time series obtained from our barometer and thermometer located at each site (the barometer and thermometer are digitized and recorded using the same recording system as the tiltmeters; gaps in these records can usually be patched by simple linear interpolation).

5. The amplitudes and phases determined in this way are converted to absolute admittances by fitting the same potential to a theoretical time series generated for the same time interval, station position and tiltmeter azimuth.

The admittances determined in this way are characteristic of a frequency band rather than a single frequency. This does not generate much of a problem in the semi-diurnal band, since most of the power in this band is at M2 and the spurious power (due to thermal or barometric pressure effects, for example) tends to be small. Thus the semi-diurnal admittance is essentially the same as the M2 admittance. This can be verified by examining the power spectrum of the residuals; the spectrum is essentially flat across the semi-diurnal band showing that a single (complex) admittance adequately fits the data. This is not the case for the diurnal band, however. We have found that effects due to barometric pressure acting on the tiltmeter are quite large here, and the spurious effects appreciably change the calculated admittance. The spectra of both temperature and barometric pressure are not sharply peaked near 1 cycle/day but have appreciable power throughout the diurnal band. As a result, our first calculated diurnal admittances were not representative of the true tidal admittance because of the admixture of temperature and pressure. Since these effects vary from month to month, the diurnal admittance was also not stable.

The stability of the semidiurnal admittance together with the contamination in the diurnal band provided a sensitive measure of the success of our efforts to isolate the instruments from spurious effects. We are pretty sure that we have essentially eliminated the sensitivity to barometric pressure by changing the design of the platform: the sensitivity to temperature has been substantially reduced by various adjustments to the electronics to minimize the overall temperature coefficient of the system.

Using the procedure outlined above, we calculated the semi-diurnal admittance for 8 consecutive months and the diurnal admittance for 2 months: we report diurnal admittances only for months when we feel the residual spurious effects were small.

The magnitude of the semi-dirunal admittance is 0.984 and the phase is -4.8 degrees. The uncertainty in the magnitude is about 6%: the corresponding uncertainty in phase is about 2.5 degrees. We feel that the admittance in the semi-diurnal band does not change by more than our quoted error across the band (i.e. that a single complex admittance can be used to describe the entire semi-diurnal response). The quoted uncertainties represent the standard deviation of the set of monthly admittances.

In the diurnal band, the amplitude of the admittance depends on the azimuth of the tiltmeter. If the azimuth of the instrument is close to 90 degrees (i.e. nominally East-West), the amplitude of the admittance is 1.2 and the phase is 4.5 degrees. The uncertainties are about 10% in amplitude and 8 degrees in phase. If the azimuth of the instrument is close to 0 degrees (i.e. nominally North-South), the admittance is smaller, but the uncertainty is large because the amplitude of the tide is quite small. We estimate that the North-South admittance is 0.9 and the phase is -5 degrees. The uncertainty is about 20% in amplitude and 15 degrees in phase, so that these numbers are not very meaningful. Note that none of our instruments is aligned exactly along either of these directions: the quoted admittances represent calculations using data whose effective azimuth was rotated using the usual rules of vector analysis.

We have obtained tidal loading calculations for Boulder from two sources. Both calculations use the Schwiderski ocean tide mode. Duncan Agnew performed calculations for the M2 and O1 tides using Goad's (1980) integrated Green's function algorithm while T. Sasao of the ILS Observatory at Mizusawa computed load effects for the M2, S2, N2, K2, K1, O1, P1, Q1 and Mf components using Farrell's (1972,1973) technique. The two calculations are in almost perfect agreement, the difference between them rarely amounting to more than 0.1 nanoradian in amplitude or 1 degree in phase. The results of these calculations are presented in table 1.

Sasao's results are most easily understood using a phasor diagram for each tidal component. Figure 1 shows his results for the M2 component and Figure 2 shows the O1 tide. The body tide and load tide vectors are shown at 12 equally spaced times during their respective tidal cycles. As can be seen from the figures, the effect of the load is quite different in the two cases. The M2 tide and load tilt vectors both rotate clockwise at approximately the same rate so that they retain a nearly constant spatial relationship. This results in a response of about 0.96 (relative to the normal body tide alone) and a phase lead of about 6 degrees with little dependence on azimuth. The

O1 tide and load vectors, however, rotate in opposite directions so that the relation between the vectors changes very rapidly with time. The response thus varies significantly with the azimuth of the tiltmeter.

Both the tide and load tilts are much larger in the East-West direction than along a North-South axis, and, for an arbitrary azimuth, the East-West tides tend to dominate the observed response. The response is greater than unity with a phase lag for most azimuths with a sharp minimum of 0.83 and large phase lead in the North-South direction.

These results are in good agreement with our measurements: the discrepancies are well within our formal statistical errors, which suggests that we have pretty well dealt with most of the spurious signals and that our instruments and our theoretical model present a consistent picture of tidal tilt.

There are, however, several noise sources that are still not too well understood. The Erie tiltmeters often report tilt glitches that are almost certainly spurious. These effects seem to be related to rainfall (but not to ground water): the effects are not the usual "tilt episodes" or tilt steps that have been reported by investigators using shallow borehole instruments. Our spurious signals consist of a series of rapid pulses: each pulse lasts about an hour. These pulses do not affect the baseline tilt (they are not steps) nor do they change the calculated admittance until they become nearly continuous. We are currently conducting a series of experiments to find our where they are coming from.

HYDROFRACTURE EXPERIMENT

On February 23, 1982, a hydrofracture experiment was performed near our Erie site by Halliburton Serivces. The company allowed us to be present on their site during the experiment and gave us all of their data.

The experiment was performed in a well that is 4856 feet deep. The well was cased with 4.5-inch diameter casing: the casing was perforated from 4838 to 4856 feet below the surface. This interval spans the 18-foot thick Shannon formation, an oil-bearing Cretaceous sandstone. Due to its relatively low permeability, this formation is routinely subjected to hydrofracture. The hydrofractures typically increase oil production by a factor of ten.

The experiment consisted of pumping a sand-laden gelled water into the well at a constant rate of 1000 gallons per minute. This high rate of injection tends to produce a narrow fracture that propagates away from the hole. The sand is used to hold the fracture open after the pumping is stopped.

At the time of the experiment, two vertical pendulum tiltmeters were operating at our site in holes number 2 and 3. These holes are both 100 feet deep. The well was 1600 feet away from the tiltmeters along an azimuth of 168 degrees. The data were recorded using our usual sampling interval of 6 minutes; the least count of the dataloggers was about 2.5 nano-radians (both of these values are typical values for all of our instruments). A four-day section of data was processed by rotating the tilt data from both instruments to azimuths along the direction of the line to the well (i.e. 168 degrees), and perpendicular to this direction. No signal related to the fracture is visible at this stage due to the much higher amplitude of the earth tides.

To remove the earth tide signal, the theoretical tidal potential was calculated for both diurnal and semi-diurnal tides. The potential was fit to the data using linear least squares. This process is much the same as the process used to calculate the tidal admittance described above, except that the data is not decimated for the hydrofracture analysis.

The residuals of these fits are shown in figures 3 and 4. On both tiltmeters, the components of tilt in line with the well tilted toward the well during the fracture. The total tilt was about 25 nano-radians. The perpendicular components are noisier, but do not show a coherent tilt signal associated with the fracture. At the conclusion of the pumping, which lasted for 84 minutes, the well was sealed at the top, and the pressure in the fracture was allowed to reach an equilibrium value over night. Any deformation recovery that occurred during this period is lost in the noise.

As this was not a controlled experiment, we do not know the parameters that are needed to completely model the deformation or the fracture geometry. No impression packer or television viewer was used to measure the strike of the fracture, and there were not enough tiltmeters at different azimuths to completely constrain the surface tilt field. We can, however, make some general estimates as to the size, extent and direction of the fracture, and some theoretical models can be used to determine if the observed tilts are at all reasonable.

In order to estimate the strike of the fracture plane, we must estimate the stress at the fracture depth. One of the principal axes of the stress tensor is usually assumed to be aligned vertically (i.e., perpendicular to the stress-free surface of the earth); the other two are in a horizontal plane. In a homogeneous medium, the fracture will open in a plane perpendicular to the axis of minimum compressive stress. The magnitude of the stress can be estimated from the pressure history of the pumping if we assume that there is negligible fluid loss (due to pre-existing cracks or to diffusion into the permeable formation, for example).

The least horizontal compressive stress is equal to the surface pressure when the pumping is first shut off. This pressure is often called the instantaneous shut-in pressure (Schnapp, et al., 1981). This pressure is the increment above hydrostatic pressure necessary to hold the fracture open. Since we are assuming that the fluid is not flowing, the pressure in the fracture is uniform. In our case, the pressure was 850 psi.

This pressure can be compared with the effective vertical stress at the fracture. The stress is equal to the lithostatic pressure of the overburden minus the original fluid pressure (Hubbert, et al., 1957). In sedimentary rock, the lithostatic pressure is typically about 1 psi/foot; the original fluid pressure is about 0.46 psi/foot. The stress at the fracture is thus approximately 4850 psi less 2231 psi or 2619 psi. Since this value is much larger than the instantaneous shut-in pressure, the fracture had to be vertical. Hubbert, et al. (1957) state that in the stress regime found in a region of normal faulting, the least principal stress will be horizontal and approximately equal to one-third of the effective vertical stress. Thus the least principal stress is approximately 2619/3 or 873 psi. This value is very close that that observed in our experiment indicating that the Erie site is in a region of extensional stress. This is consistent with the data of Zoback and Zoback (1980), who place the Erie site in the Southern Great Plains stress province, a region in a state of uniform extensional stress extending from Western Texas to Northeastern Colorado. They report that the direction of least principal stress is along an azimuth of about 45 degrees based on studies of earthquakes induced by fluid injection at the nearby Rocky Mountain Arsenal. This suggests that the Erie fracture was near vertical and probably had a strike along an azimuth of 135 degrees assuming that there were no modifications due to local structure.

The extent and width of the fracture may be estimated using a theoretical model given by Sun (1969). This model was developed for a circular disk-shaped fracture in an infinite, linear, isotropic, homogeneous medium. The hydraulic pressure is assumed to be applied uniformly over the entire surface of the fracture. The radius of the fracture is given by:

$$r = \left[\frac{3\mu V}{8 P_f (1-\nu)}\right]^{1/3}$$

where

μ=2000000 psi=shear modulus for sedimentary rock;

V=112000 cubic feet=volume of injected fluid;

ν =0.25=Poisson's ratio;

P_f =Pressure in the fracture.

The maximum separation of the fracture, W, is given by:

$$W = \frac{4 P_f (1-\nu) r}{\pi \mu}$$

Evans, et al., (1980), explain that the appropriate value for P_f is the driving pressure, the additional pressure required to open and extend the fracture. It is equal to the fluid pressure in the fracture minus the in situ stress normal to the fracture.

Although the density of the injection fluid was increased in six steps, the fluid pressure in the crack remained fairly constant at 3230 psi during the entire pumping time. The driving pressure is then about 150 psi giving a fracture radius of 418 feet and a maximum width of 0.35 inches. The surface area is thus about 549000 square feet.

The actual shape of the fracture is unlikely to be a simple circle considering the high injection pressure, but these values can be used as a guideline for further modeling.

Dr. Tom Dobecki of Fracture Technology, Inc. has kindly computed the surface tilts to be expected in our situation. The calculation is done analytically using a program written by Dr. Paul Davis of UCLA. The analytic solution predicts tilts on the order of 20 - 40 nano-radians at our instruments. The relationship between the fracture axis and the tilt axis is different, however. Although the details of the solutions depend on the detailed values of the parameters, the character of the solutions does not. The axis of the fracture is essentially perpendicular to the axis of maximum tilt. Since our instruments showed essentially no tilt along an axis perpendicular to the azimuth of the well, our data combined with this model would yield an azimuth of about 78 degrees for the fracture with an uncertainty of about 15 degrees. This is not consistent with the picture of the stress field as presented by Zoback and Zoback (1980). However, a closer inspection of Zoback and Zoback shows that the Erie site is in fact in a transition zone between the Great Plains and the Southern Rocky Mountain provinces: the principal axis in the latter tend to be aligned along a more nearly North-South azimuth, and it is not unreasonable to expect an intermediate azimuth in the transition zone. Since we do not have sufficient azimuthal coverage, there is not enough data to constrain the solution for the azimuth of the fracture. The magnitude of the tilt step is, however, consistent with the analytical model.

YELLOWSTONE ARRAY

During the period covered by this report, we also completed the design for the array of tiltmeters to be installed in Yellowstone National Park.

The array consists of five pairs of holes located at Tower Junction, Norris, Madison, Lake and Canyon. All of the holes are nominally 100 feet deep: the holes all have double casing with cement between the outer and inner casings. The outer casing was needed to prevent the hole from closing behind the drill bit. The holes should be much better than those at Erie since they will be totally dry. (When only one casing is used, it must be forced into the hole after the drilling is completed. In several cases, the pressure needed to force the casing into the hole produced cracks in the welds between the casing sections. These cracks allowed water to leak in over the tiltmeter.) The size of the inner casing and the design of the bottom section of the hole are the same as in our previous installations.

Each site is equipped with a datalogger consisting of a small micro-computer and associated analog to digital converter. A dial telphone has also been installed at each site. We intend to access each site via direct distance dialing from Boulder approximately once per day. Using this system, all sites are totally independent of each other: a failure anywhere can only disable a single site. This is an important advantage, since much of the array will be very difficult to get to during the winter months.

In addition to storing the data from the tiltmeters at each site, some of the dataloggers will be equipped with sensors to monitor atmospheric pressure and temperature. The Physical Science Coordinator in the park is also interested in correlating our tide data with other measurements, and some form of data sharing will be arranged.

We have made three trips to the Park this year, and almost all of the site preparation is complete. The only exception is Norris, where we have not yet been able to get telephone service. Telephone serivce there may not be available until next year.

We are planning a fourth trip to Yellowstone during the last week of September to install two additional tiltmeters. We will then have three tiltmeters installed: one each at Lake, Canyon and Tower. We expect to begin recording data from all of these instruments by the middle of October.

CONCLUSIONS

We have compared the measured tidal admittances obtained using tilt data at our two sites with theoretical calculations: we find good agreement both in the semi-diurnal and diurnal bands, although the uncertainties in the estimate of the measured diurnal admittance are too large to make possible a rigorous comparison of theory and experiment.

The diurnal tide shows some residuals effects due to spurious effects and we are continuing to improve our instruments so as to reduce the sensitivity of the tiltmeters to fluctuations in ambient temperature or pressure.

We have compared the tilt-step observed during a nearby hydro-fracture experiment with the step expected on the basis of average regional geology. We find good agreement on the magnitude of the step: the data and the theory seem to diagree on the azimuth of the fracture, but neither the theory nor the measurements are sufficiently robust to allow us to evaluate the significance of the discrepancy.

We have completed the design of our Yellowstone array, and we have begun installing tiltmeters. We hope to have three tiltmeters running with completed data telemetry before the roads close for the winer.

REFERENCES

Goad, Clyde C., Gravimetric Tidal Loading Computed from Integrated Green's Functions, J. G. R., 85, 2679-83, (1980).

Evans, K. F., The Growth and Consolidation Characteristics of Shallow Hydraulic Fractures as Viewed through the Surface Deformation Field, SPE/DOE 10851 (1982).

Evans, K. F., G. R. Holzhausen and M. D. Wood, The Mapping of Nitrogen Gas Induced Hydraulic Fractures in Devonian Shale by Observation of Associated Surface Deformation, SPE/DOE 8933, Symposium on Unconventional Gas Recovery, 18 - 20 May 1980, Pittsburgh, Pa.

Farrell, W. E., Deformation of the Earth by Surface Loads, Rev. Geophys. Space Phys., 10, 761-97 (1972).

Farrell, W. E., Earth Tides, Ocean Tides and Tidal Loading, Phil. Trans. Roy. Soc. London, A274, 253-9, (1973).

Hubbert, M. K. and D. G. Willis, Mechanics of Hydraulic Fracturing, Trans. AIME, 210, 153-68, (1957).

Schnapp, M., J. G. Hocherhaus and R. A. Nelson, Stress Measurements in Salt in a Deep Borehole in Southeastern Utah, J. G. R., in press (1982).

Sun, R. J., Theoretical Size of Hydraulically Induced Horizontal Fractures and Corresponding Surface Uplift in an Idealized Medium, J. G. R., 74, 5995-6011 (1969).

Zoback, M. L. and M. D. Zoback, State of Stress in the Conterminous United States, J. G. R., 85, 6113-52 (1980).

TABLE 1

TILT TIDE AT BOULDER INCLUDING LOADING
Tilts in Nano-radians

Comp	Az (deg)	Body Tide	Load Tide	Total Tide	Response Mag.	Response Phase(deg)
M2	90	40.35	3.62	39.14	0.97	-4.9
S2	90	18.82	0.35	18.91	1.00	-1.0
N2	90	7.73	0.82	7.01	0.91	-3.2
K2	90	5.11	0.14	5.03	0.98	-1.3
M2	0	25.94	3.95	24.67	0.95	-8.5
S2	0	12.10	1.80	11.91	0.98	-8.6
N2	0	4.97	0.88	4.56	0.92	-9.4
K2	0	3.29	0.55	3.22	0.98	-9.6
K1	90	19.79	5.19	23.88	1.20	+8.4
O1	90	14.06	3.15	16.91	1.20	+5.0
P1	90	6.55	1.58	7.79	1.19	+7.7
Q1	90	2.69	0.54	3.20	1.19	+3.2
K1	0	5.33	1.45	4.70	0.88	-15.4
O1	0	3.79	1.06	3.14	0.83	-16.4
P1	0	1.77	0.46	1.51	0.85	-16.9
Q1	0	0.73	0.23	0.56	0.77	-16.3

FIGURE CAPTIONS

Fig. 1. Sasao's results for the effect of loading on the M2 component of the tilt tide at Boulder. The outer ellipse shows the amplitude of the body tide as a function of the azimuth of the observing instrument. The M2 body tide moves along the outer ellipse, making one revolution per M2 period. The inner circle shows the M2 load (magnified by 2X for visibility). The load is omnidirectional and rotates in the same direction as the body tide. The phase relationship between the two is therefore essentially constant. The numbers around the periphery of each trace show the corresponding points for the body and load tides at the same time. The amplitude and phase of the resultant admittance (relative to the body tide) are plotted for several azimuths.

Fig. 2. Sasao's results for the effect of loading on the O1 component of the tilt tide at Boulder. The outer ellipse shows the amplitude of the body tide as a function of the azimuth of the observing instrument. The O1 body tide moves along the outer ellipse, making one revolution per O1 period. The inner ellipse shows the O1 load. The body and load vectors rotate in opposite directions around their respective ellipses in contrast to the M2 case. The amplitude of the measured tide therefore changes rapidly with azimuth. The amplitude and phase of the resultant admittance (relative to the body tide) are plotted for several azimuths.

Fig 3. Residuals obtained after a least-squares estimte of the tidal tilt is subtracted from the tilt data at Erie. The x-axis is in days and the y-axis is in nanoradians. The residuals have been rotated to an azimuth of 168 degrees (nominally along a line between the instruments and the test well). The two traces show the data from two independent two-axis instruments in holes number 2 and 3 of our Erie site.

Fig. 4. Residuals obtained in the same way as figure 3 except that the data have been rotated to an azimuth of 78 degrees (nominally perpendicular to the line between the instruments and the test well).

M_2 TILT

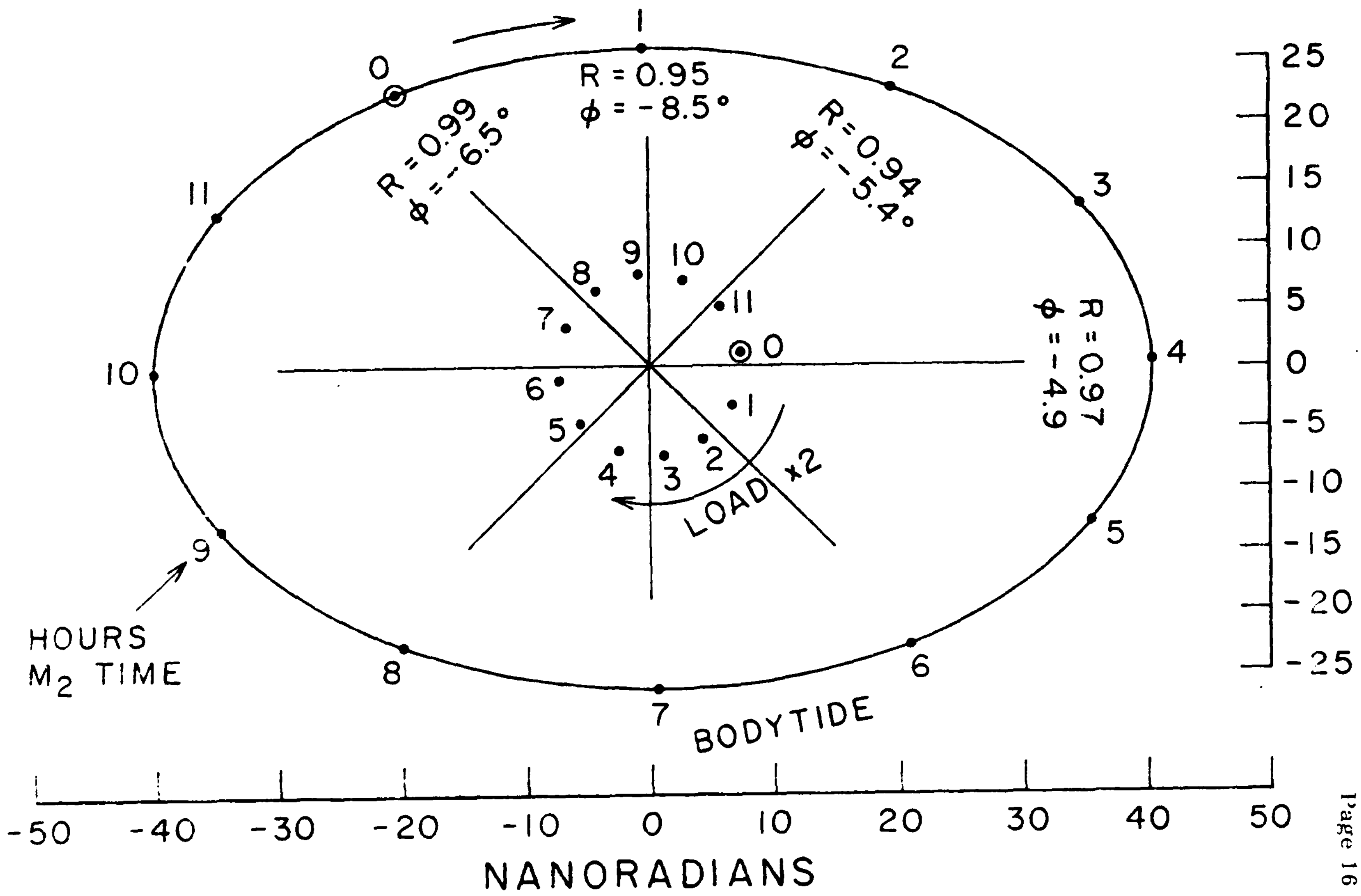
R = 0.95
φ = -8.5°
R = 0.99
φ = -6.5°
R = 0.94
φ = -5.4°
R = 0.97
φ = -4.9
LOAD x2
BODYTIDE
HOURS
M2 TIME
25
20
15
10
5
0
-5
-10
-15
-20
-25
-50
-40
-30
-20
-10
0
10
20
30
40
50
NANORADIANS

O_1 TILT

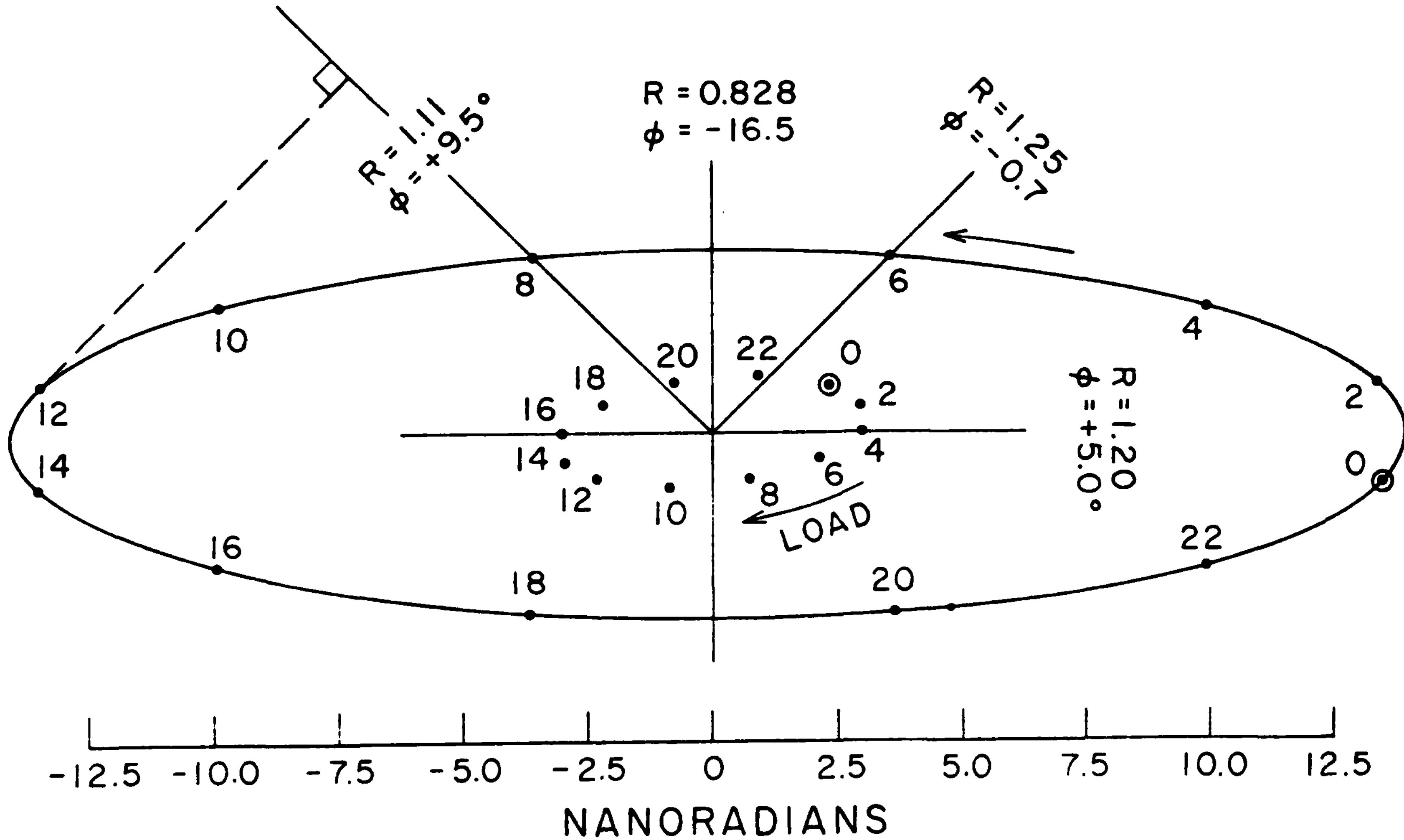
R = 0.828
φ = -16.5
R = 1.11
φ = +9.5°
R = 1.25
φ = -0.7
R = 1.20
φ = +5.0°
LOAD
0
2
4
6
8
10
12
14
16
18
20
22
-12.5
-10.0
-7.5
-5.0
-2.5
0
2.5
5.0
7.5
10.0
12.5
NANORADIANS

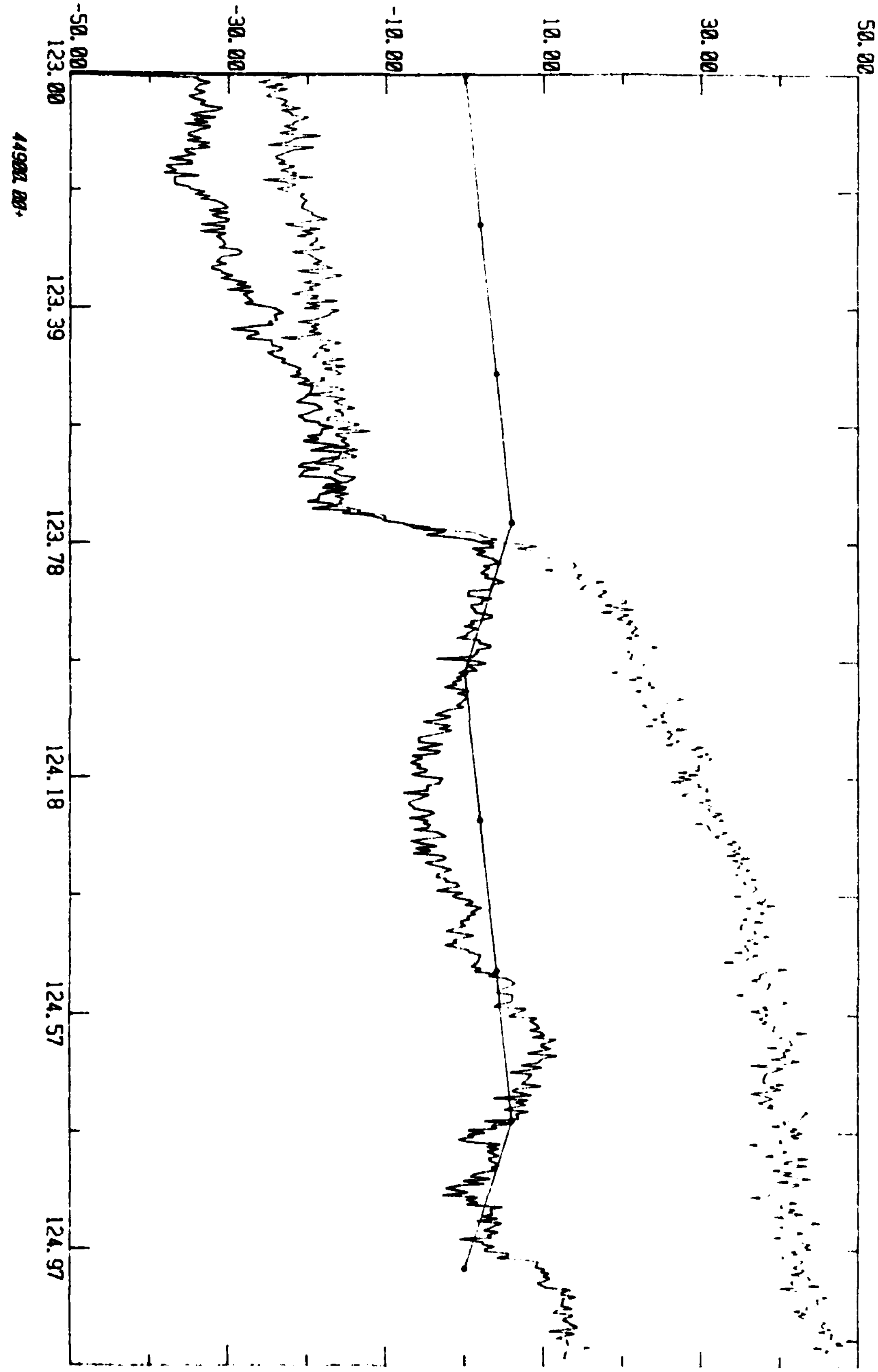

-50.00
-30.00
-10.00
10.00
30.00
50.00
123.00
123.39
123.78
124.18
124.57
124.97
44900.00+

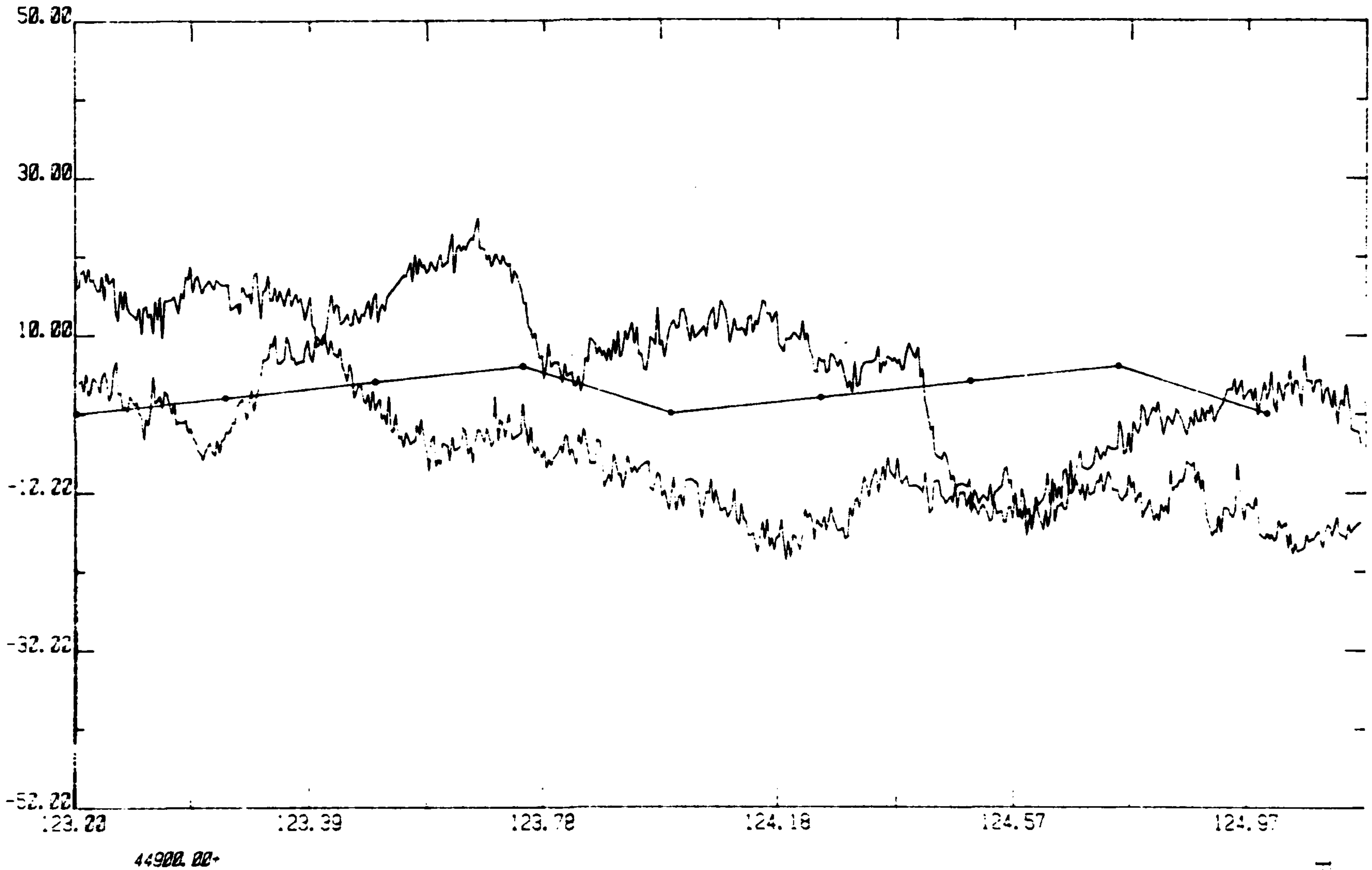

50.00
30.00
10.00
-12.22
-32.22
-52.22
123.23
123.39
123.78
124.18
124.57
124.97
44900.00+

FILMED

1-83

DTIC